Multi scale numerical approach for micro-cracked viscoelastic masonry

T.T.Nga Nguyen [1,*], *S.Tuan* Nguyen[2], *N.Quang* Vu[1], *T.Ta.Nguyen[1]*, *N.Hung* Tran[1] and *M. Ngoc* Vu[2]

[1] ITSE, Le Quy Don Technical University, Ha Noi, Viet Nam
[2] IRD, Duy Tan University, 03 Quang Trung, Da Nang, Vietnam

Abstract. A multi-scale numerical method for viscoelastic micro-cracked masonry is proposed. Firstly, the effective viscoelastic properties of the masonry are modelled by a periodic homogenization approach. The Modified Maxwell (MM) model is chosen for the creep. Secondly, an incremental procedure is proposed. Thirdly, an incremental formulation is used to get the overall viscoelastic behaviour of the two dimensional periodic cell. Finally, the result of the method is validated against analytical solution.

1 Introduction

In recent year, more and more high buildings are being constructed in developing countries such as Vietnam. These structures are explicitly required to withstand the movement induced by wind and earthquake. They are also expected to avoid the occurrence of severe damage within non-structural elements which can cause risks for people living inside the building as well as the main structure. Masonry infill is known as the building envelope with or without load-bearing role. Indeed, infill walls contribute significantly to the stiffness and resistance of the building. The experimental and analytical results indicate that the infill masonry can remarkably improve the performance of reinforced concrete or steel frames [1-3] and that the probability of failure of the frames with regularly distributed infill is much smaller than that of the bare frame [4-6]. To avoid irreparable damage and catastrophic failure, efficient methods for modelling and predicting mechanical deformations of infill masonry walls are strongly needed.

In addition, the non-linear phenomena occurred in masonry infill must be adequately considered in the design of masonry infilled RC frame for the model to be realistic. Creep strains should be taken into account because it significantly contributes towards the material properties of masonry [7]. Similar to the concrete and other materials, at constant stress, the masonry exhibits viscoelastic behaviour [8-11]. Effectively, the nonlinear mechanical behaviour for the masonry is due to the creep behaviour of the mortar [12]. Among a number of rheological models examined to predict the creep of mortar, the

* Corresponding author: thungaxd@yahoo.com

Modified Maxwell model is likely the most accurate and will be used in this paper to describe the mortar joint's creep [11].

Besides, the decay in material properties may occur in masonry due to cracking. Micro-cracks appear lead to the loss of the load bearing capacity of masonry structure which can be accompanied by a facilitation of main structure collapse in dynamic loads (earthquake, blasting load, for example). This is especially important for high buildings, which consist of RC frame structure and masonry infill.

The goal of this paper is to provide a finite element procedure for micro-cracked viscoelastic masonry. In Section 2, the basis of the periodic approach for effective viscoelastic properties of fractured masonry is reported. Section 3 describes a finite element procedure to determine the effective behaviour of micro-cracked viscoelastic masonry. The accuracy of the results is verified by a preliminary comparison with existent results in the case without crack. An infilled frame structure containing micro-cracked viscoelastic masonry will be modelled in Section 4. The role of masonry infill on the whole structure will be discussed in section 5.

2 Periodic approach

This section describes a periodic approach based on finite element simulation to determine the viscoelastic properties of masonry. Mechanical properties of masonry depend on the mechanical properties of components (bricks and mortar) and their arrangement, in which the brick is supposed to be uncracked and elastic while the mortar is described by Modified Maxwell (MM) linear viscoelastic model (see Fig. 1). Obviously, MM might be properly able to represent the creep behaviour of masonry ages at loading (see [11]).

Following the micro-macro approach, Anthoine [13] firstly used finite element method (FEM) applied on a REV to obtain the macroscopic properties of masonry. However, his work was limited in the elastic behaviour of two components. This study focuses on the micro-macro approach where an extension of FEM for the viscoelastic behaviour will be developed. However, this model cannot be applied directly to masonry in which the mortar is micro-cracked and linear viscoelastic. The Laplace-Carson (LC) transform is used to transform the behaviour non-aging linear viscoelastic (NALV) of the component from the real-time space to linear elastic one in symbolic space. .

Nguyen et al. [14] modelled the effective behaviour of a NALV cracked concrete, in which the cement is represented by the Burger model, by using the coupling between the homogenization method and Griffith's theory. In the symbolic space, the displacement jump is linearly dependent on the macroscopic stress (dilute scheme) and the behaviour of micro-cracked viscoelastic concrete still follows the same class of model (i.e. Burgers) in the short and long terms. The originality of this work is that we can use this idea to define effective linear viscoelastic behaviour of micro-cracked mortar with Modified Maxwell (MM) model which then has to be used in the periodic homogenization of the heterogeneous masonry.

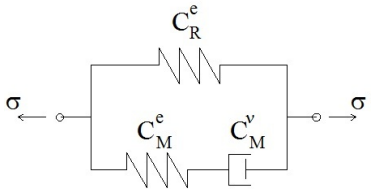

Fig. 1. Rheological model for mortar

2.1 Basic of the periodic approach

In most cases of building practice, bricks and mortar are periodically arranged. A micro-macro approach of homogenization bases on three steps. The first step is to define a REV. We are reminded that the choice of REV is not unique [13, 15, 16]. A good choice can reduce the computational cost. As the considered basic cell plane is symmetrical to two axes, the study can be carried out on a quarter cell with ordinary boundary conditions resulting from the combination of periodicity and symmetry (see Fig. 2).

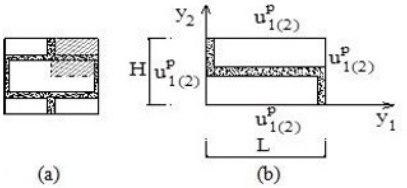

Fig. 2. A chosen REV (a) and its quarter (b)

Then, the second step consists in analysing the local consequence of a global load in terms of stress and strain fields in the REV. By applying a uniform displacement load at the edge of REV (see Fig. 3), Nguyen et al. [14] noted that the macroscopic stress is an average of the stress field in REV as follows:

$$\Sigma = \bar{\sigma} = \frac{1}{S}\int_S \sigma ds \tag{1}$$

with S is the total area of REV. Eq. (1) can be rewritten by:

$$\Sigma = \varphi^m \bar{\sigma}^m + \varphi^b \bar{\sigma}^b \tag{2}$$

Where φ^m, φ^b are respectively volume fractions of mortar and bricks; $\bar{\sigma}^m$, $\bar{\sigma}^b$ are the averages of the stress in mortar and bricks.

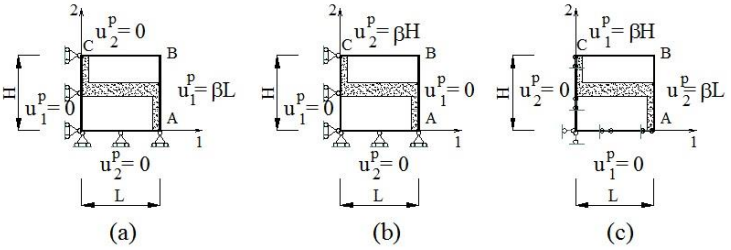

Fig. 3. Periodic boundary conditions at the edges of a quarter cell. Simple displacement u along the first axis (a), the second axis (b) and simple shear (c)

The last step is homogenization to obtain the effective properties of a homogeneous medium equivalent to the considered heterogeneous REV from the properties of components and their arrangement. Under the plane stress assumption, the macroscopic tensor of elastic stiffness has five independent coefficients to be determined (for more detail, see [13, 18]). Then, equivalent elastic moduli $\tilde{E}_{ij}$ and Poisson's ratios ν_{ij} are derived by:

$$\tilde{\mathrm{C}} = \begin{pmatrix} \tilde{C}_{1111} & \tilde{C}_{1122} & 0 \\ \tilde{C}_{2211} & \tilde{C}_{2222} & 0 \\ 0 & 0 & \tilde{C}_{1212} \end{pmatrix} = \frac{1}{1-\nu_{12}\nu_{21}} \begin{pmatrix} \tilde{E}_{11} & \nu_{21}\tilde{E}_{11} & 0 \\ \nu_{12}\tilde{E}_{22} & \tilde{E}_{22} & 0 \\ 0 & 0 & \tilde{\mu}_{12}\left(1-\nu_{12}\nu_{21}\right) \end{pmatrix} \tag{3}$$

2.2 Modified Maxwell model for uncracked viscoelastic mortar

The rheological MM model described the viscoelastic behaviour of mortar reads:

$$\mathrm{S}_M^v\,\sigma+\mathrm{S}_M^e\,\dot{\sigma}=\ \mathrm{S}_M^v\,\mathrm{C}_R^e\,\varepsilon+\left(\mathrm{I}+\ \mathrm{S}_M^e\ \mathrm{C}_R^e\right)\dot{\varepsilon} \tag{4}$$

where $\mathrm{S}_M^v, \mathrm{S}_M^e, \mathrm{C}_R^e,\ \mathrm{C}_R^e$ are model's parameters given in [18].

In the symbolic space of LC, Eq. (4) is linear:

$$\mathrm{S}_M^v\,\sigma^*+p\ \mathrm{S}_M^e\,\sigma^*=\ \mathrm{S}_M^v\,\mathrm{C}_R^e\,\varepsilon^*+p\left(\mathrm{I}+\ \mathrm{S}_M^e\ \mathrm{C}_R^e\right)\varepsilon^* \tag{5}$$

Since the apparent "stress-strain" relation (5) can be written as $\sigma^*=\mathrm{C}^*\,\varepsilon^*$ with $\mathrm{C}^*=3k_s^*\mathrm{J}+2\,\mu_s^*\mathrm{K}$, so the apparent bulk and shear moduli for the uncracked mortar can be written as follows:

$$k_s^*=\frac{1}{\dfrac{1}{k_M^e}+\dfrac{1}{p_M^s/3}}+k_R^e,\qquad \mu_s^*=\frac{1}{\dfrac{1}{\mu_M^e}+\dfrac{1}{p_M^d/2}}+\mu_R^e \tag{6}$$

Replacing $\dot{a}$ byits approximation $\dot{a}\cong\dfrac{a(t+dt)-a(t)}{dt}$ in Eq. (4) results in

$$\left(c_5\mathrm{J}+c_6\mathrm{K}\right)\sigma(t+dt)-\left(c_7\mathrm{J}+c_8\mathrm{K}\right)\sigma(t)=\left(c_1\mathrm{J}+c_2\mathrm{K}\right)\varepsilon(t+dt)-\left(c_3\mathrm{J}+c_4\mathrm{K}\right)\varepsilon(t) \tag{7}$$

with:

$$\begin{gathered}c_1=\frac{3k_R^e}{\underset{M}{s}}+\frac{1}{dt}\left(1+\frac{k_R^e}{k_M^e}\right),\ c_2=\frac{2\mu_R^e}{\underset{M}{d}}+\frac{1}{dt}\left(1+\frac{\mu_R^e}{\mu_M^e}\right),\ c_3=\frac{1}{dt}\left(1+\frac{k_R^e}{k_M^e}\right),\ c_4=\frac{1}{dt}\left(1+\frac{\mu_R^e}{\mu_M^e}\right),\\ c_5=\frac{1}{\underset{M}{s}}+\frac{1}{dt}\frac{1}{3k_M^e},\ c_6=\frac{1}{\underset{M}{d}}+\frac{1}{dt}\frac{1}{2\mu_M^e},\ c_7=\frac{1}{dt}\frac{1}{3k_M^e},\ \ c_8=\frac{1}{dt}\frac{1}{2\mu_M^e}\end{gathered} \tag{8}$$

2.3 Effective properties of micro-cracked viscoelastic mortar

According to Nguyen et al. [14, 19], the apparent effective bulk and shear moduli of concrete are obtained in the symbolic space by a combination of the Eshelby-based homogenization scheme and the Griffith's theory:

$$\frac{1}{\tilde{k}_{d_c}^*}=\frac{1+d_cQ^*}{k_s^*}\ \text{with}\ Q^*=\frac{16}{9}\frac{1-v_s^{*2}}{1-2v_s^*};\ \frac{1}{\tilde{\mu}_{d_c}^*}=\frac{1+d_cM^*}{\mu_s^*}\ \text{with}\ M^*=\frac{32}{45}\frac{\left(1-v_s^*\right)\left(5-v_s^*\right)}{2-v_s^*} \tag{9}$$

where k_s^*, μ_s^*, v_s^* are respectively the apparent bulk, shear moduli and Poisson's ratio of the uncracked mortar. d_c is crack density parameter defined by $d_c=N.l^3$; N is number of cracks per unit of volume and l is radius of the cracks.

Then, the inversion of the LC transform (ILC) is required to determine the effective behaviour in the temporal real space. The presence of cracks makes the formula of moduli to be complex, hence the ILC is carried out exactly only in some simple cases by calculating the integral of Bromwich [20]. It is interesting to approach in the symbolic space the symbolic effective moduli by the ones of an existing rheological model, at least in short and long terms. Nguyen et al. [14] suggested using the same model of the uncracked concrete for the cracked one. In this study, the similar idea is followed to the mortar. We will try to approach the cracked mortar by the MM model (for more detail, see [18, 21]). We have the effective stiffness and viscosity parameter related to the MM model:

$$\frac{1}{k_M^e(\mathrm{d_c})}=\frac{1+Q_M^e\mathrm{d_c}}{k_R^e+k_M^e-\dfrac{k_R^e(1+Q_M^e\mathrm{d_c})}{1+Q_M^\nu\mathrm{d_c}}},\ \frac{1}{k_R^e(\mathrm{d_c})}=\frac{1+Q_M^\nu\mathrm{d_c}}{k_R^e},\ \frac{1}{\mu_M^e(\mathrm{d_c})}=\frac{1+M_M^e\mathrm{d_c}}{\mu_R^e+\mu_M^e-\dfrac{\mu_R^e(1+M_M^e\mathrm{d_c})}{1+M_M^\nu\mathrm{d_c}}},$$

$$\frac{1}{\mu_R^e(\mathrm{d_c})}=\frac{1+M_M^\nu\mathrm{d_c}}{\mu_R^e},\ \frac{1}{\eta_M^s(\mathrm{d_c})}=\frac{(1+Q_M^\nu\mathrm{d_c})^2}{\eta_M^s(1+Q_M^\nu\mathrm{d_c})-3\mathrm{d_c}k_R^eQ_1^0},\ \frac{1}{\eta_M^d(\mathrm{d_c})}=\frac{(1+M_M^\nu\mathrm{d_c})^2}{\eta_M^d(1+M_M^\nu\mathrm{d_c})-2\mathrm{d_c}\mu_R^eM_1^0} \quad (4)$$

where Q_α^β , M_α^β are given in Nguyen et al. [18]. For each value of crack density parameter d_c , characteristics of cracked mortar are determined by (10). The viscoelastic properties of hybrid mortar with or without cracks are given in Table 1.

Table 1. The effective properties of hybrid mortar

d_c	$k_M^e(d_c)$ (MPa)	$\mu_M^e(d_c)$ (MPa)	$\eta_M^s(d_c)$ (MPa.s)	$\eta_M^d(d_c)$ (MPa.s)	$k_R^e(d_c)$ (MPa)	$\mu_R^e(d_c)$ (MPa)
0.0	2404	1655	3.35 108	1.54 108	1257	866
0.1	1846	1440	2.57 108	1.33 108	965	754
0.2	1498	1275	2.09 108	1.19 108	784	667

3. The finite element procedure

3.1. The incremental procedure

Levin et al., [22] presented a theorem that can address the homogenization of linear elastic materials with pre-stress or initial deformation. Follow this theorem, macroscopic stress field at the time (t+dt) is written in the form:

$$\sigma(t+dt)=\mathrm{C}_{MM}^{INC}:\varepsilon(t+dt)+\sigma_{MM}^p(t) \quad (11)$$

with $\sigma_{MM}^p(t)$ the pre-stress, which concern the stress and strain at time t and given by:

$$\sigma_{MM}^p(t)=-\left(\frac{c_3}{c_5}\mathrm{J}+\frac{c_4}{c_6}\mathrm{K}\right)\varepsilon(t)+\left(\frac{c_7}{c_5}\mathrm{J}+\frac{c_8}{c_6}\mathrm{K}\right)\sigma(t) \quad (12)$$

and the stiffness tensor of viscoelastic mortar: $\mathrm{C}_{MM}^{INC}=\frac{c_1}{c_5}\mathrm{J}+\frac{c_2}{c_6}\mathrm{K}$, where

$$c_1=\frac{3k_R^e}{\eta_M^s}+\frac{1}{dt}(1+\frac{k_R^e}{k_M^e}),\quad c_2=\frac{2\mu_R^e}{\eta_M^d}+\frac{1}{dt}(1+\frac{\mu_R^e}{\mu_M^e}),\ c_3=\frac{1}{dt}(1+\frac{k_R^e}{k_M^e}),\quad c_4=\frac{1}{dt}(1+\frac{\mu_R^e}{\mu_M^e})$$

$$c_5=\frac{1}{\eta_M^s}+\frac{1}{dt}\frac{1}{3k_M^e},\quad c_6=\frac{1}{\eta_M^d}+\frac{1}{dt}\frac{1}{2\mu_M^e},\ c_7=\frac{1}{dt}\frac{1}{3k_M^e},\quad c_8=\frac{1}{dt}\frac{1}{2\mu_M^e}$$

For the incremental algorithm, we effectuate as follows:

+ At t=0s, instant response is elastic, only the elastic parts of the spring and Maxwell contribute to the rigidity of the material. The constitutive law is: $\sigma_1=\mathrm{C}_{MM1}^{INC}:\varepsilon_1$ with $\mathrm{C}_{MM1}^{INC}=\mathrm{C}_{RM}^e=\mathrm{C}_R^e+\mathrm{C}_M^e$.

+ At t = dt, the relation between σ_2 and ε_2 reads: $\sigma_2=\mathrm{C}_{MM2}^{INC}:\varepsilon_2+\sigma_{MM1}^p$ where the pre-stress σ_{MM1}^p given by eq. (12) corresponding to the stress σ_1 and the strain ε_1 .

The creep behaviour of a hollow sphere is now considered to validate the incremental procedure. This sphere, constituted by a porous material, is subjected to a traction on the

edge l_3 and fictive press mass on the edge l_1 that gives the nodal force P (see Fig. 4-a). The macroscopic strain is determined by: $\bar{\varepsilon} = \varphi\bar{\varepsilon}^p + (1-\varphi)\bar{\varepsilon}^s$ where φ is the volume fraction of the porous phase, $\bar{\varepsilon}^s$, $\bar{\varepsilon}^p$ are respectively the average strains of the solid phase and porous phase:

$$\bar{\varepsilon}^s = \frac{1}{\Omega^s}\int_{\Omega^s}\frac{tr(\varepsilon)}{3}d\Omega,\ \bar{\varepsilon}^p = \frac{P.U}{3.\Omega^p} \tag{13}$$

with U the nodal displacement vector, Ω^s and Ω^p are the volumes of the solid phase and porous phase, respectively. The strain for the elastic case is determined analytically by the relation: $\bar{\varepsilon} = \frac{\Sigma_0}{3.k(\varphi)}$ where $k(\varphi)$ is the effective bulk modulus estimated by Hashin's model: $k(\varphi) = k_s^e\left(1-\varphi\frac{3k_s^e+4\mu_s^e}{3\varphi k_s^e+4\mu_s^e}\right)$ (see [23]). As the material is linear viscoelastic, the strain is obtained by the inverse LC transform of this equation: $\bar{\varepsilon}^* = \frac{\Sigma_0}{3.k^*(\varphi)}$ with $k^*(\varphi) = k_s^*\left(1-\varphi\frac{3k_s^*+4\mu_s^*}{3\varphi k_s^*+4\mu_s^*}\right)$; k_s^* and μ_s^* are given by (6). When dt is small enough (ie. $dt = 10^4\ s$), we have a very good validation between two calculations (see Fig. 4-b).

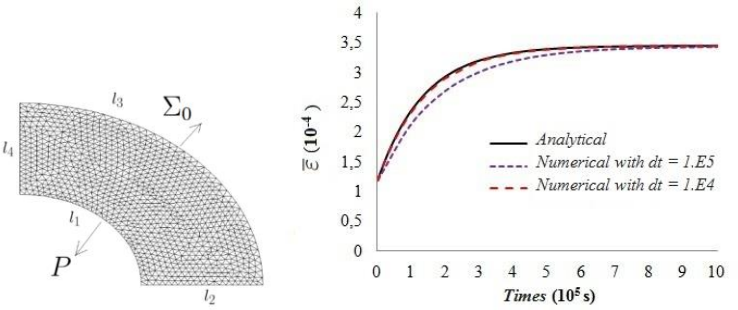

(a) (b)

Fig. 4. A hollow sphere with a volume factor $\varphi = 0.125$ under $\Sigma = 1MPa$ (a) and validation of the incremental procedure (b), $d_c = 0.0$.

3.2. The numerical approach for two dimensional REV

The calculations of stress and strain are carried out step by step with the finite element method for $dt = 10^4\ s$, using the rheological behaviour law of mortar (i.e. Modified Maxwell) through an incremental formulation. It should be noted that the relationship between the pre-stress σ_{MM}^p expressed at previous time t in the mortar and the fictive nodal force P is:

$$P = \mathrm{A}^m : \sigma_{MM}^p \tag{14}$$

with A^m transformation from stress into forces in the mortar. σ_{MM}^p is then transformed into fictive nodal force on the mortar. This force is then considered as an external force on the mortar in addition to displacement load at the edge of REV. Therefore, the overall

behaviour of the periodic cell is elastic for each step of the time and written in the following form:

$$\bar{\sigma}_{\text{cell}}\left(t+dt,d_c\right)=\tilde{\mathrm{C}}_{cell}\left(t+dt,d_c\right):\bar{\varepsilon}_{cell}\left(t+dt,d_c\right) \tag{15}$$

In this relation, variables are function of the crack density and time.

Besides, Cecchi and Tralli [12] proposed a multi-parameter analytical homogenization study for the two-dimensional uncracked viscoelastic masonry. In this way, the reduction of joints to interfaces is based on the hypothesis of rigid bricks (which is suitable when bricks generally much stiffer than mortar) and small thickness of mortar compared with bricks. The viscoelastic behaviour is also only observed in mortar joints. It is useful to use this analytical approach to validate the numerical approach.

The geometric dimensions and the mechanical characteristics of elastic bricks are: 250x250x55 (mm3), $E^b=15.5\,10^6$ (MPa) [24]. A good agreement between the present work and analytical calculation of [12] are showed in Fig. 5 for simple uncracked case where the bricks are much stiffer than the mortar and the thickness of mortar joint is very small (i.e. 2 mm).

It is then possible to evaluate the following properties of a periodic masonry cell (2D) with micro-cracked viscoelastic mortar $d_c=0.1$, $e^m=10\,(\text{mm})$, $E^b=\infty$, $\nu^b=0.2$ under the assumption of plane stress. We see in Table 2 that when t exceeds 11 days, effective modules tend to a finite asymptotic limit.

Table 2 The effective properties of REV

Time(days)	$\tilde{\tilde{E}}_1$ (MPa)	$\tilde{\tilde{E}}_2$ (MPa)	$\tilde{\tilde{G}}_{12}$ (MPa)	$\tilde{\nu}_{12}$	$\tilde{\nu}_{21}$
0	9761	9257	3821	0.196	0.186
1	8823	7250	2914	0.191	0.156
7	8312	6066	2405	0.186	0.136
11	8305	6060	2403	0.185	0.135

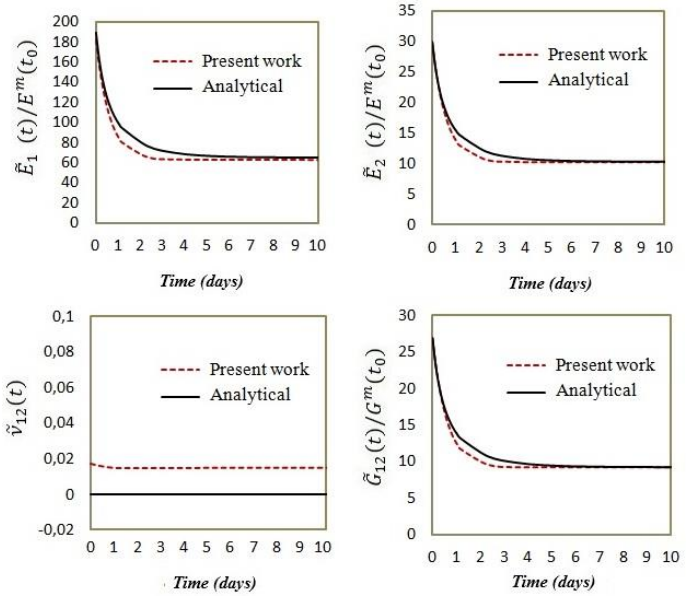

Fig. 5. Comparison of effective modules and coefficient of a masonry derived from numerical and analytical models in uncracked case. The modules and viscosity coefficients of hybrid mortar are presented in Table 1.

4 Conclusions

This work provides a numerical tool to predict the effective behavior of a 2D periodic masonry with micro-cracked viscoelastic mortar and elastic brick. MM model is used to represent the mortar behaviour. An FEM incremental procedure was described to compute the effective properties of the assemblage of bricks and mortar. A comparison between the results obtained from the analytical and numerical approaches for two dimensional REV showed that the presented procedure gives reliable results. Future work will focus on crack propagation that is still limited in this study and the numerical model will be developed by using mortar-brick nonlinear interface. This study should be improved for other creep models and some examples of the masonry infilled frame test should also be simulated using this proposed model to show good agreement with experimental results.

This research is funded by Vietnam National Foundation for Science and Technology Development (NAFOSTED) under grant number 107.01-2017.307.

References

1. A. Saneinejad, B. Hobbs, JOSE, **121**, 4 (1995).
2. A.B. Mehrabi, P. Benson Shing, M.P. Schuller, J.L. Noland, JSENDH, **122**, 3 (1996)
3. W. W. El-Dakhakhni, M. Elgaaly, A. A. Hamid, JSENDH, **129**, 2 (2003)
4. C. V. R. Murty, S. K. Jain, *12WCEE*, (2000)
5. M. Dolšek, P. Fajfar, Eng. Struct., **30**, 7 (2008)
6. O. Bolea, (2016). Energy Procedia, **85**, 60 (2016)
7. S. Ignoul, L. Schueremans, L. Binda, *Of the 5th int. seminar on SAHC*, **2**, 913 (2006)
8. N. G. Shrive, E. Y. Sayed-Ahmed, D. Tilleman, Can. J. Civ. Eng., **24(3)**, 367 (1997)
9. B. Vandoren, K. Heyens, K. De Proft, Complas (2011)
10. E. Verstrynge, L. Schueremans, D. Van Gemert, Mater. Struct., **44(1)**, 29 (2011)
11. K. K. Choi, S. L. Lissel, M. M. Reda Taha, Can. J. Civ. Eng., **34(11)**, 1506 (2007)
12. A. Cecchi, A. Tralli, Int. J. Solids Struct., **49**, 1485 (2012)
13. A. Anthoine, Int. J. Solids Struct., **32(2)**, 137 (1995)
14. S.T. Nguyen, L. Dormieux, Y.L. Pape, J. Sanahuja, Int.J. Damage Mech., **20(8)**, 1116(2011)
15. A. Cecchi, K. Sab, Eur. J. Mech. A. Solids, **21(2)**, 249 (2002)
16. A. Cecchi, K. Sab, Eur. J. Mech. A. Solids, **21(5)**, 715 (2002)
17. R. Luciano, E. Sacco, Eur. J. Mech. A. Solids, **17(4)**, 599 (1998)
18. T. T. N. Nguyen, A. Rekik, A. Gasser, *WCCM XI*, 3381 (2014)
19. S. T. Nguyen, Doc. Diss., (2010)
20. S. Beurthey, A. Zaoui, Eur. J. Mech. A. Solids, **19(1)**, 1 (2000)
21. T.N.Nguyen, S.T. Nguyen, M.H. Vu, M.N. Vu, Int.J. Damage Mech., **25(4)**, 557 (2016)
22. V. Levin, M. Markov, S. Kanaun, J. Geophys. Res. B: Solid Earth, **109** (2004)
23. L. Dormieux, D. Kondo, F. J. Ulm, *Microporomechanics*, John Wiley & Sons, (2006)
24. A. Orduña, P. B. Lourenço, Int. J. Solids Struct., **42(18)**, 5161 (2005)